© 2017. Published by The Company of Biologists Ltd | Development (2017) 144, 2092-2097 doi:10.1242/dev.145805

TECHNIQUES AND RESOURCES

RESEARCH REPORT

Optimized CUBIC protocol for three-dimensional imaging of chicken embryos at single-cell resolution

María Victoria Gómez-Gaviro[1,2,3,‡,§], Evan Balaban[4,*,‡], Diana Bocancea[1], María Teresa Lorrio[1], Maria Pompeiano[4,*], Manuel Desco[1,2,3], Jorge Ripoll[1,2] and Juan José Vaquero[1,2]

ABSTRACT

The CUBIC tissue-clearing protocol has been optimized to produce translucent immunostained whole chicken embryos and embryo brains. When combined with multispectral light-sheet microscopy, the validated protocol presented here provides a rapid, inexpensive and reliable method for acquiring accurate histological images that preserve three-dimensional structural relationships with single-cell resolution in whole early-stage chicken embryos and in the whole brains of late-stage embryos.

KEY WORDS: Tissue clearing, 3D imaging, Chicken embryo, Light-sheet microscopy

INTRODUCTION

The easy accessibility and physiological independence of chicken embryos have made them an important biological model system for over a century in the fields of developmental biology, neurobiology, genetics, immunology, cancer, virology, cardiovascular and cell biology (Stern, 2005). Recent chicken embryo work has revealed dynamic gene expression patterns underlying somite formation (Pourquié, 2004; Davey and Tickle, 2007), unexpectedly large variations in embryonic brain regional metabolic activity during the last 20% of *in ovo* development (Balaban et al., 2012), and no coordinated patterns of brain gene expression resembling adult sleep or waking (Chan et al., 2016).

To better exploit the potential of chicken embryos for simultaneously examining electrophysiological, metabolic and molecular correlates of the brain-wide development of neural network activity, it is necessary to adapt methods that can rapidly and efficiently detail the structure and gene expression of developing networks in three dimensions with single-cell resolution. This was not achieved by previous three-dimensional (3D) technologies such as optical coherence tomography and photoacoustic tomography (Wong et al., 2013; Liu et al., 2014).

Optical imaging of tissue samples is limited by visible-range light scattering. While penetration depths of up to 1 mm have been achieved with two-photon microscopy (Theer et al., 2003), conventional confocal microscopy remains limited to 100 µm (Poguzhelskaya et al., 2014; Nehrhoff et al., 2016). This requires large tissue samples to be cut into thinner sections, resulting in both tissue geometry distortion and loss of precise 3D morphology. New tissue-clearing methods enable the analysis of thicker samples (Susaki et al., 2014) that are well suited for new volumetric imaging modalities such as light-sheet microscopy (Ripoll et al., 2015; Arranz and Ripoll, 2015). The CLARITY method clears mouse brains yet retains immunohistochemical compatibility (Chung et al., 2013), providing a way to acquire 3D images with single-cell resolution without having to cut specimens into thin sections. We present a validated protocol for whole chicken embryos and whole chicken embryonic brains using modifications of an alternative tissue-clearing method – the CUBIC (clear, unobstructed brain imaging cocktails and computational analysis) method of Susaki et al. (2014, 2015) – combined with a light-sheet microscope adapted to generate 3D quantitative images with single-cell resolution.

RESULTS AND DISCUSSION

We modified, optimized and validated the CUBIC technique on early whole chicken embryos and late-stage chicken embryo brains, and assessed the impact of clearing on sample transparency, size, and cellular and subcellular tissue integrity using computed tomography (CT) imaging and confocal, light-sheet and electron microscopy.

It is well known that embryonic tissue differs from that of adult organisms, both in the type and the number of cells, and in chemical composition. Although 6 days of incubation in the lipid-removing Reagent 1 were necessary to clear adult mouse brains, 2 days were sufficient to achieve a highly transparent sample for late-stage chicken embryo brains of similar size (Fig. 1A,B) and 4 h for early-stage whole embryos (Fig. 1C,D,G). Transparency in embryo brains was compared with a widely used clearing protocol for light-sheet microscopy imaging: benzyl alcohol benzyl benzoate (BABB) (Genina et al., 2010). BABB and CUBIC achieved similar transparency (Fig. 2A).

CUBIC was initially reported to cause swelling after immersion of the sample in Reagent 1; this effect was reduced after sucrose dehydration steps (Susaki et al., 2015). Changes in the weight of isolated late-stage chicken embryo brains treated with either BABB or CUBIC were assessed before and after clearing. BABB significantly reduced chicken embryo brain weight by an average of ∼25%, whereas CUBIC resulted in a non-significant increase of less than 10% in average brain weight (Fig. 2B). For a subset of embryo brains, CT images were taken before and after clearing. Data analysis revealed a highly significant correlation between changes in brain weight and changes in brain volume ($r=0.94$, $P<0.0001$, $n=13$; Fig. 2C). BABB significantly decreased brain weight and brain volume, whereas CUBIC resulted in non-significant increases in both weight and volume (Fig. 2C). This indicates that brain

[1]Departamento de Bioingeniería e Ingeniería Aeroespacial, Universidad Carlos III de Madrid, Leganés, 28911, Spain. [2]Instituto de Investigación Sanitaria Gregorio Marañón, Madrid, 28007, Spain. [3]Centro de Investigación Biomédica en Red de Salud Mental (CIBERSAM), Madrid, 28029, Spain. [4]Department of Psychology, McGill University, Montreal, QC H3A 1B1, Canada.
*Present address: Departamento de Bioingeniería e Ingeniería Aeroespacial, Universidad Carlos III de Madrid, Leganés, 28911, Spain.
‡These authors contributed equally to this work

§Author for correspondence (vgomez@hggm.es)

M.V.G.-G., 0000-0002-8683-5150; M.D., 0000-0003-0989-3231; J.R., 0000-0001-8856-7738; J.J.V., 0000-0001-9200-361X

Received 25 January 2017; Accepted 7 April 2017

Development (2017) 144, 2092-2097 doi:10.1242/dev.145805

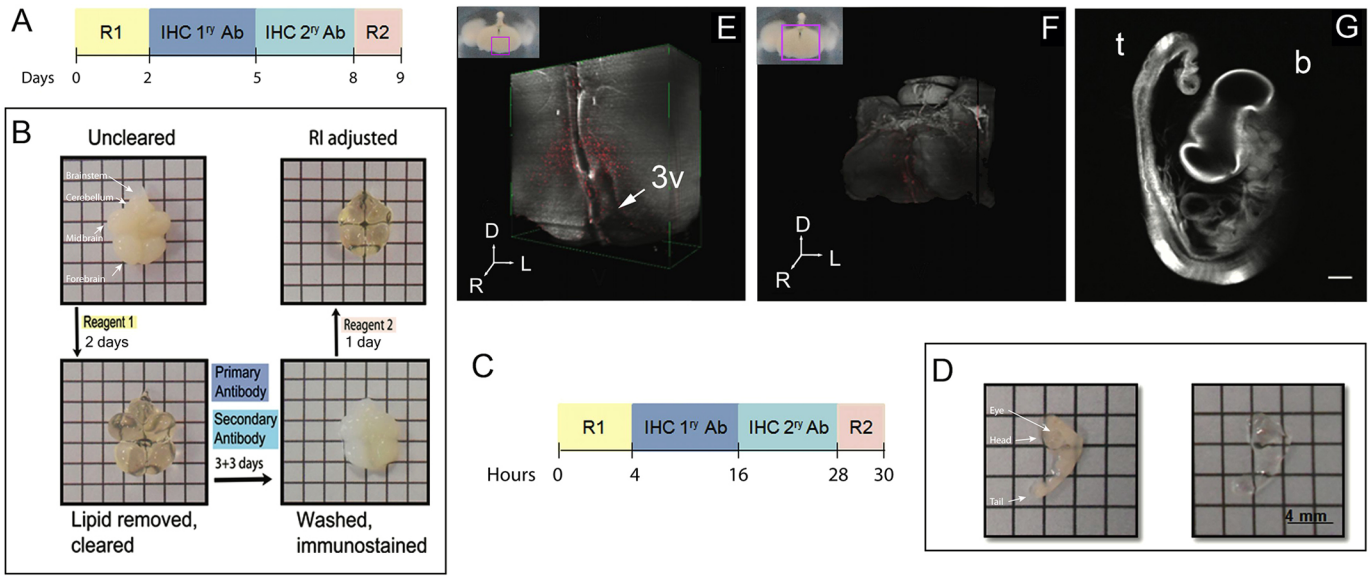

Fig. 1. Chicken embryo clearing. (A) Schedule for chicken embryo brain clearing and immunostaining. (B) Appearance of an E16 brain after each protocol step. Brains become transparent after treatment with Reagent 1, opaque when washed and immunostained, and transparent again after incubation with Reagent 2. (C) Schedule for whole chicken embryo clearing and immunostaining. (D) Untreated (left) and cleared (right) E4 embryos. (E,F) Light-sheet microscopy fluorescent images of an E16 whole brain (insets are a representative brain slice that illustrates the location of the main images). Red, orexinergic neuron bodies; grey, DAPI. (G) Mid-sagittal view of a whole E4 chicken embryo. 3v, third ventricle; Ab, antibody; b, brain; D, dorsal; IHC, immunohistochemistry; L, lateral; R, rostral; R1 and R2, Reagent 1 and Reagent 2; RI, refraction index; t, tail. Scale bars: 4 mm in D; 1 mm in G.

weight changes during the clearing process are a reliable proxy for brain volumetric changes.

In CUBIC-treated brains, general tissue morphology [assessed with Hematoxylin and Eosin (H&E) staining] was well maintained at cellular and subcellular levels of resolution, even though much of the tissue lipid content was lost (Fig. 2D). Transmission electron microscopy (TEM) revealed that subcellular structures were largely preserved, even though the relative lack of lipids resulted in decreased image contrast [Fig. 2E, Fig. S1; previously described by Susaki et al. (2014); the osmium tetroxide used for TEM staining binds to lipids to enhance image contrast; Reagent 1 removes lipids, decreasing osmium tetroxide binding, so that the image contrast also decreases]. In summary, the CUBIC protocol employed here maintains the general integrity of cellular and tissue structures, increasing brain volume ∼3-10% on average, whereas BABB shrinks brain volumes by ∼20-30%. These results agree with similar measurements using BABB-cleared and CUBIC-cleared mouse embryos and embryonic heart tissue (Kolesová et al., 2016).

Entire brains from embryos incubated for 16 days (E16) were cleared with the optimized CUBIC methodology and triple immunostained to show orexin and catecholaminergic (TH-positive) neurons and cFos-active nuclei, with DAPI counterstaining to identify all cell nuclei. These staining combinations were previously used by Landry et al. (2014, 2016) and Chan et al. (2016) in chicken embryos and post-hatched chicks. Light-sheet microscopy of the CUBIC-cleared brains produced images with sufficient resolution to clearly recognize single labelled cells in the hypothalamus (Fig. 1E,F, Movies 1-8), as well as to follow their labelled neuronal processes (Fig. S3). A similar protocol was developed for E4 whole chicken embryos, with shorter incubation times (Fig. 1C).

Compatibility with confocal microscopy was assessed using 1-mm thick sections of chicken embryo brain. We investigated whether penetration depth could be increased by clearing. High transparency was achieved in thick tissue sections after immersion in Reagent 1 for 4 h (see Fig. 4A). This treatment enabled incubation times to be reduced to 1 day for each of the primary and secondary antibody solutions. A penetration depth of 500 µm was achieved with a 10× objective and a depth of ∼150 µm was achieved with a 20× objective (Fig. 3A). By contrast, uncleared control sections produced more light scattering, which limited penetration to ∼100 µm with a 10× objective. To confirm that the penetration depth was limited by light scattering rather than insufficient antibody penetration, the 1 mm sections were sliced into ∼150 µm sections along their *z*-axis. Positive TH and DAPI signals were obtained from all five thin slices throughout the depth of the *z*-axis, confirming that the antibodies fully penetrated the 1 mm section (Fig. 3B). Taken together, these results demonstrate that an optimized CUBIC protocol can also be used for thick tissue sections with confocal microscopy.

To confirm that the optimized CUBIC-clearing and immunostaining protocol provides comparable results to standard histology and immunohistochemistry, we compared our results with those of Godden et al. (2014), Landry et al. (2014, 2016) and Chan et al. (2016). The stained cells obtained with our optimized protocol showed identical spatial distributions to those obtained in these previous studies at both E16 (Fig. 4C,D; orexinergic neurons are also shown in Fig. S4, Movie 6) and at E20 (Movie 8).

In conclusion, the validated CUBIC method proposed here represents an important resource facilitating future chicken embryo imaging studies, and provides a powerful combination of clearing and immunostaining compatible with both 3D laser-sheet microscopy and confocal imaging that can be used for studying DNA, RNA and protein expression patterns, neuronal connectivity, and subcellular-to-systems brain morphology at single-cell resolution.

MATERIALS AND METHODS

Egg incubation and sample preparation

Fertilized chicken eggs were incubated in standard conditions. Immersion-fixed E4 whole chicken embryos and perfusion-fixed E16, E18 and E20

Development (2017) 144, 2092-2097 doi:10.1242/dev.145805

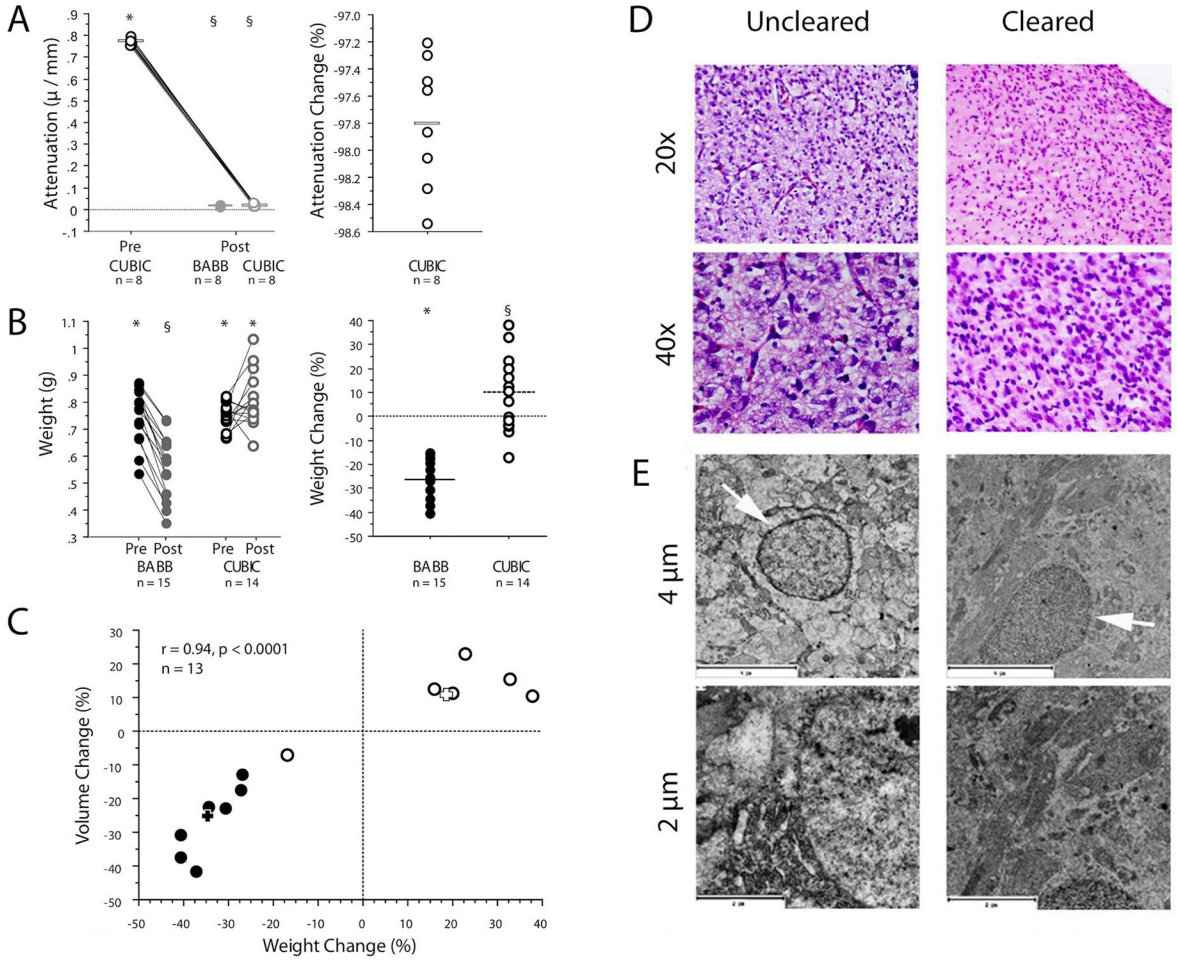

Fig. 2. CUBIC and BABB clearing of chicken embryo brains. (A,B) Symbols above graphs denote statistically significant differences; groups with different symbols are significantly different from each other. Bars indicate mean. (A) Light attenuation in CUBIC brains [*n*=8; measured before (open circles with black border) and after (open circles with grey border) clearing] and BABB brains [*n*=8; only measured after clearing (grey filled circles)]. (Left) CUBIC brains showed a highly significant reduction in light attenuation after clearing: before 0.77±0.01 (s.e.m.), after 0.017±0.001 μ/mm (Wilcoxon matched pairs sign-rank test, 8/8 differences <0, z=−2.521, *P*=0.012). After clearing, the attenuation coefficients of BABB-cleared and CUBIC-cleared brains were not significantly different from each other (Mann–Whitney *U*-test, U=31, U′=33, z=−0.105, *P*=0.92). (Right) Percentage change in light attenuation of CUBIC-cleared brains (mean, −97.79±0.17%). (B) Weight of E16 chicken embryo brains before and after clearing. (Left) Scheirer-Ray-Hare two-way ANOVA with method [BABB (filled circles) versus CUBIC (open circles)] and time [before clearing (black fill or border) versus after clearing (grey fill or border)] as factors. This analysis indicated a significant overall difference due to method (H=10.75, d.f.=1, *P*=0.001), no significant difference due to time (H=3.48, d.f.=1, *P*=0.062), and a significant method-time interaction (H=12.69, d.f.=1, *P*=0.0003). Wilcoxon matched pair post-hoc tests corrected for multiple comparisons indicated that BABB samples significantly decreased in weight [before 0.75±0.03, after 0.55±0.03 g (15/15 differences <0, z=−3.41, *P*=0.0014)], whereas CUBIC samples did not [before 0.75±0.01, after 0.81±0.03 g (8/14 differences <0, z=−1.73, *P*=0.17)]. There was no significant difference between BABB and CUBIC weights prior to clearing (Mann–Whitney *U*-test corrected for multiple comparisons, U=96, U′=114, z=−0.39, *P*>0.95), whereas there was a significant difference after clearing (U=6, U′=204, z=−4.3, *P*<0.0001). (Right) Percentage change in the weight of BABB-cleared (mean, −26.49±2.25%) and CUBIC-cleared (mean, 8.96±4.23%) brains. The two methods had significantly different percentage weight changes (Mann–Whitney *U*-test, U=2, U′=208, z=−4.49, *P*<0.0001). (C) The relationship between brain weight change and volume change. The final 13 brains [seven BABB (solid black circles), six CUBIC (white circles)] processed for measurement in B were subjected to CT imaging before and after clearing and their 3D volumes calculated from the CT images. There was a highly significant correlation between the percentage weight change (*x*-axis) and the percentage volume change (*y*-axis) (r=0.94, *n*=13, *P*<0.0001). Black plus sign indicates mean BABB value (weight change, −33.93±2.22%; volume change, −26.62±3.99%); white plus sign indicates mean CUBIC value (weight change, 18.79±2.22%; volume change, 10.83±4.10%). BABB and CUBIC samples had significantly different weight changes (Mann–Whitney *U*-test, U=0, U′=42, z=−3.00, *P*=0.0027) and volume changes (Mann–Whitney *U*-test, U=0, U′=42, z=−3.00, *P*=0.0027). The BABB brains showed significant changes post-clearing in both weight and volume (Wilcoxon matched pairs sign-rank test corrected for multiple comparisons, both variables 7/7 differences <0, z=−2.37, *P*=0.036), whereas the CUBIC brains did not show significant changes in either weight or volume (Wilcoxon matched pairs sign-rank test corrected for multiple comparisons, both variables 1/6 differences <0, z=−1.99, *P*=0.093). (D) H&E staining of CUBIC-cleared and uncleared chicken embryo brains. Images were acquired with 20× and 40× objectives. Cytoplasm and nuclear staining appear generally preserved after clearing. (E) Subcellular resolution observed by TEM in cleared (right) and uncleared (left) chicken embryo brain. Membrane integrity was preserved in uncleared fixed brains and less so in the cleared fixed brains. Arrows indicate membranes (top) that are shown at higher magnification (bottom). Scale bars: 4 μm (top), 2 μm (bottom).

chicken embryo brains were obtained. 1-mm thick coronal sections were obtained by cutting perfusion-fixed brains using a vibrating microtome (7000smz-2, Campden Instruments, Loughborough, UK) and were collected in rostral-to-caudal order (Fig. 4A,B). For further details, see the supplementary Materials and Methods.

Optimized CUBIC clearing protocol

Brains were incubated in Reagent 1 in a shaker for 2 days at 37°C at 80 rpm and then washed with PBS three times for 2 h each at room temperature. Thereafter, they were dehydrated for 30 min in 20% sucrose in PBS and then incubated in Reagent 2 for 1 day at 37°C and 80 rpm. Incubation times in

Development (2017) 144, 2092-2097 doi:10.1242/dev.145805

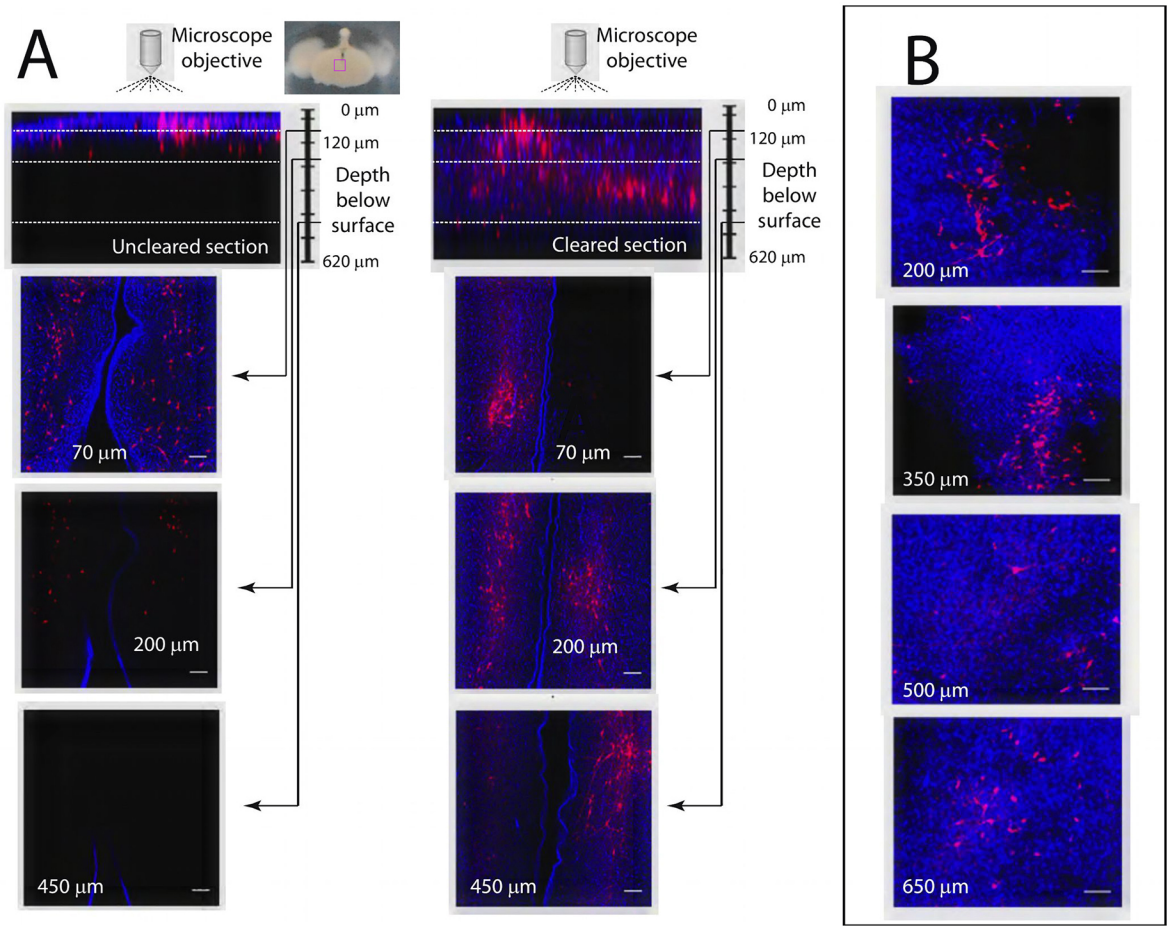

Fig. 3. The optimized clearing protocol improves penetration of laser light and antibodies into thick brain sections for confocal microscopy. (A) Confocal images of thick (1 mm) hypothalamic sections in an E16 chicken embryo brain (inset is a representative brain slice that illustrates the location of the main images). Images were obtained from untreated (left) and cleared (right) sections at different depths, as indicated. (B) Antibody penetration in cleared sections. Cleared thick sections were sliced (150 µm, vibratome) and visualized by confocal microscopy to determine the depth of antibody penetration (*z*-axis). Blue, DAPI-stained nuclei; red, TH-positive neuron bodies. 10× objective. *z*-stack step size, 23 µm. Scale bars: 100 µm for all images.

Reagent 1 and 2 were reduced for whole embryos (to 4 h and 2 h, respectively) and 1-mm thick sections (4 h each). Solutions are described in the supplementary Materials and Methods.

Transparency measurements

The transparency of brains cleared with the optimized CUBIC and BABB (as in Genina et al., 2010) protocols was compared by conventional light microscopy. Detailed measurement information is provided in the supplementary Materials and Methods.

CT imaging

The volumes of brains cleared with the optimized CUBIC and the BABB protocols were measured using an Argus PET/CT preclinical scanner (SEDECAL, Madrid, Spain). Details are provided in the supplementary Materials and Methods.

H&E staining and TEM

H&E staining to assess general tissue morphology was performed as described in the supplementary Materials and Methods. For ultrastructural analyses, optimized CUBIC-cleared and uncleared brains were postfixed in osmium tetroxide and potassium ferricyanide, and ultrathin sections prepared and examined by TEM using a JEOL 1230 microscope (IZASA Scientific, Madrid, Spain) (for details, see the supplementary Materials and Methods).

Immunostaining

Fluorescent immunostaining and optimized CUBIC clearing protocols were integrated for chicken embryo brains (Fig. 1A). Brains were incubated in Reagent 1 (containing DAPI; Invitrogen; 1:5000) for 2 days, washed, then incubated in primary antibody solution (anti-orexin, anti-TH and anti-cFos antibodies; together, each at 1:250) in a shaker for 3 days at 37°C and 80 rpm. After washes, the fluorescent secondary antibody solution (each at 1:300) was applied for 3 days at 37°C and 80 rpm. Brains were then washed, dehydrated in sucrose solution and finally incubated in Reagent 2 for 1 day. Similar protocols were developed with reduced incubation times in the two antibody solutions for early-stage whole chicken embryos (12 h each; Fig. 1C) and 1-mm-thick sections (1 day each). Primary and secondary antibodies are listed in Table S1.

Light-sheet microscopy

Immunostained brains were analyzed with a custom-made light-sheet microscope. Information about the set-up, image acquisition and processing are provided in the supplementary Materials and Methods, Fig. S2 and Table S2.

Confocal microscopy

An inverted confocal microscope (Leica TCS SPE) was used. Confocal images from 1-mm thick coronal sections were acquired and processed as described in the supplementary Materials and Methods.

Acknowledgements

We thank Jesús Amo Aparicio, Alexandra de Francisco and Yolanda Sierra for sample preparation; Rafael Samaniego for confocal image acquisition; Fernando Escolar (CIB, CSIC) for subcellular imaging; and COBB Española S.A. for providing the fertilized eggs.

Development (2017) 144, 2092-2097 doi:10.1242/dev.145805

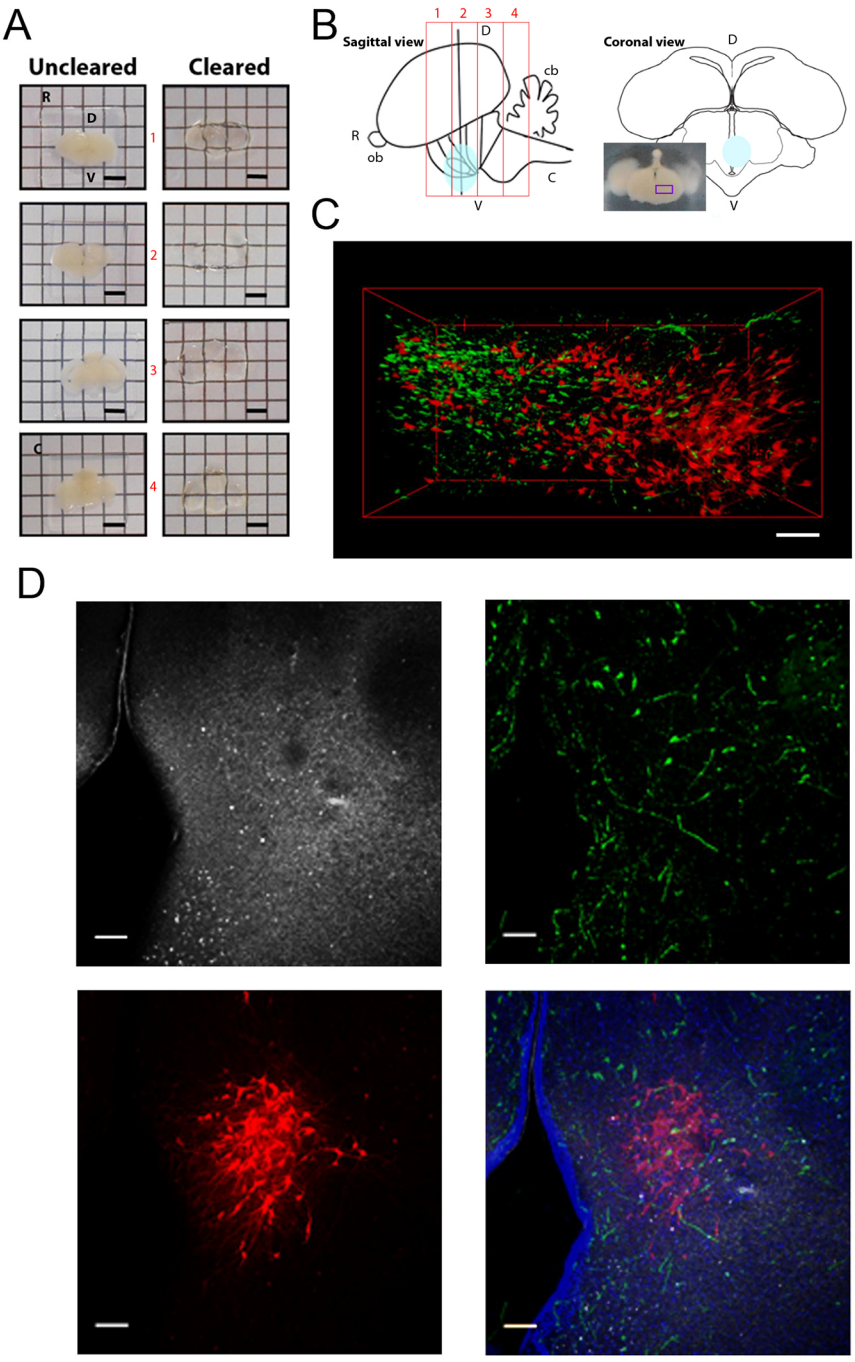

Fig. 4. CUBIC clearing and immunostaining imaging of thick sections from E16 chicken embryo brains. (A) Four consecutive rostral (R) to caudal (C) sections [red rectangles (left to right) in B] from a brain before (left) and after (right) CUBIC clearing. (B) Schematic sagittal and coronal brain sections showing the hypothalamic region imaged in D (light blue); inset is a representative brain slice that illustrates the location of the image in C. C, caudal; cb, cerebellum; D, dorsal; ob, olfactory bulb; R, rostral; V, ventral. (C) 3D volumetric rendering of neurons in the hypothalamus. Red, TH-positive neurons; green, orexinergic neurons. 10× objective. (D) Confocal images of the same hypothalamic region obtained with different filters. Grey, cFos-positive nuclei (top left); green, orexinergic neurons (top right); red, TH-positive neurons (bottom left); merge, with DAPI-stained nuclei in blue (bottom right). 10× objective. *z*-stack step size, 23 µm. Scale bars: 3 mm in A; 100 µm in D.

Competing interests
The authors declare no competing or financial interests.

Author contributions
Conceptualization: M.V.G., E.B., M.P., J.R., J.J.V.; Methodology: M.V.G., E.B., D.B., M.T.L., M.P., M.D., J.R., J.J.V.; Software: D.B., M.T.L., J.R.; Validation: M.V.G., E.B., J.J.V.; Formal analysis: M.V.G., E.B., D.B., M.P., M.D.; Investigation: M.V.G., E.B., M.T.L., J.R., J.J.V.; Resources: J.R., J.J.V.; Data curation: M.D.; Writing - original draft: M.V.G.; Writing - review & editing: M.V.G., E.B., M.P., M.D., J.R., J.J.V.; Visualization: E.B., M.D., J.R., J.J.V.; Supervision: E.B., J.R., J.J.V.; Project administration: E.B., J.J.V.; Funding acquisition: E.B., J.J.V.

Funding
The study was supported by the Human Frontier Science Program (RGP0004/2013), the European Commission Seventh Framework Programme (FP7, EU CIG Grant), the Ministerio de Economía y Competitividad (FIS2013-41802-R) and Consejería de Educación, Juventud y Deporte, Comunidad de Madrid (P2013/ICE 2958).

Supplementary information
Supplementary information available online at
http://dev.biologists.org/lookup/doi/10.1242/dev.145805.supplemental

References
Arranz, A. and Ripoll, J. (2015). Advances in optical imaging for pharmacological studies. *Front. Pharmacol.* **6**, 189.
Balaban, E., Desco, M. and Vaquero, J. J. (2012). Waking-like brain function in embryos. *Curr. Biol.* **22**, 852-861.
Chan, A., Li, S. H., Lee, A. R., Leung, J., Yip, A., Bird, J., Godden, K. E., Martinez-Gonzalez, D., Rattenborg, N. C., Balaban, E. et al. (2016). Activation of state-

Development (2017) 144, 2092-2097 doi:10.1242/dev.145805

regulating neurochemical systems in newborn and embryonic chicks. *Neuroscience* **339**, 219-234.

Chung, K., Wallace, J., Kim, S.-Y., Kalyanasundaram, S., Andalman, A. S., Davidson, T. J., Mirzabekov, J. J., Zalocusky, K. A., Mattis, J., Denisin, A. K. et al. (2013). Structural and molecular interrogation of intact biological systems. *Nature* **497**, 332-337.

Davey, M. G. and Tickle, C. (2007). The chicken as a model for embryonic development. *Cytogenet. Genome Res.* **117**, 231-239.

Genina, E. A., Bashkatov, A. N. and Tuchin, V. V. (2010). Tissue optical immersion clearing. *Expert Rev. Med. Devices* **7**, 825-842.

Godden, K. E., Landry, J. P., Slepneva, N., Migues, P. V. and Pompeiano, M. (2014). Early expression of hypocretin/orexin in the chick embryo brain. *PLoS ONE* **9**, e106977.

Kolesová, H., Čapek, M., Radochová, B., Janáček, J. and Sedmera, D. (2016). Comparison of different tissue clearing methods and 3D imaging techniques for visualization of GFP-expressing mouse embryos and embryonic hearts. *Histochem. Cell Biol.* **146**, 141-152.

Landry, J. P., Hawkins, C., Wiebe, S., Balaban, E. and Pompeiano, M. (2014). Opposing effects of hypoxia on catecholaminergic locus coeruleus and hypocretin/orexin neurons in chick embryos. *Dev. Neurobiol.* **74**, 1030-1037.

Landry, J. P., Hawkins, C., Lee, A., Coté, A., Balaban, E. and Pompeiano, M. (2016). Chick embryos have the same pattern of hypoxic lower-brain activation as fetal mammals. *Dev. Neurobiol.* **76**, 64-74.

Liu, M., Maurer, B., Hermann, B., Zabihian, B., Sandrian, M. G., Unterhuber, A., Baumann, B., Zhang, E. Z., Beard, P. C., Weninger, W. J. et al. (2014). Dual modality optical coherence and whole-body photoacoustic tomography imaging of chick embryos in multiple development stages. *Biomed. Opt. Express* **5**, 3150-3159.

Nehrhoff, I., Bocancea, D., Vaquero, J., Vaquero, J. J., Ripoll, J., Desco, M. and Gómez-Gaviro, M. V. (2016). 3D imaging in CUBIC-cleared mouse heart tissue: going deeper. *Biomed. Opt. Express* **29**, 3716-3720.

Poguzhelskaya, E., Artamonov, D., Bolshakova, A., Vlasova, O. and Bezprozvanny, I. (2014). Simplified method to perform CLARITY imaging. *Mol. Neurodegener.* **9**, 19.

Pourquié, O. (2004). The chick embryo: a leading model in somitogenesis studies. *Mech. Dev.* **121**, 1069-1079.

Ripoll, J., Koberstein-Schwarz, B. and Ntziachristos, V. (2015). Unleashing optics and optoacoustics for developmental biology. *Trends Biotechnol.* **33**, 679-691.

Stern, C. D. (2005). The chick: a great model system becomes even greater. *Dev. Cell* **8**, 9-17.

Susaki, E. A., Tainaka, K., Perrin, D., Kishino, F., Tawara, T., Watanabe, T. M., Yokoyama, C., Onoe, H., Eguchi, M., Yamaguchi, S. et al. (2014). Whole-brain imaging with single-cell resolution using chemical cocktails and computational analysis. *Cell* **157**, 726-739.

Susaki, E. A., Tainaka, K., Perrin, D., Yukinaga, H., Kuno, A. and Ueda, H. R. (2015). Advanced CUBIC protocols for whole-brain and whole-body clearing and imaging. *Nat. Protoc.* **10**, 1709-1727.

Theer, P., Hasan, M. T. and Denk, W. (2003). Two-photon imaging to a depth of 1000 µm in living brains by use of a Ti:Al_2O_3 regenerative amplifier. *Opt. Lett.* **28**, 1022-1024.

Wong, F., Welten, M. C. M., Anderson, C., Bain, A. A., Liu, J., Wicks, M. N., Pavlovska, G., Davey, M. G., Murphy, P., Davidson, D. et al. (2013). eChickAtlas: an introduction to the database. *Genesis* **51**, 365-371.